NUMERICAL STUDY OF NORMAL IMPINGEMENT OF A PLANE JET ON A FLAT SURFACE

by K. SANKARA RAO, *Applied Mathematics Section, Vikram Sarabhai Space Centre, Trivandrum* 695022

(*Received* 18 *April* 1975)

Numerical solutions to the problem of unsteady plane incompressible viscous jet impinging on to an infinite flat surface are presented in this paper for Reynolds number = 450 using Dufort-Frankel implicit scheme. Steady state solutions were obtained for Reynolds number = 450 and for Prandtl's number = 1. Static pressure distribution, shear stress and Nusselt number distribution on the flat surface are shown graphically for various values between nozzle to plate spacing. Streamlines and equivorticity lines are also drawn. The results of our investigation are in qualitative agreement with those available in the literature.

1. INTRODUCTION

The prediction of base flow characteristics when a free jet strikes a flat surface is of interest in many practical problems such as paint sprays, shield-arc welding and jet-blast, particularly in connection with current schemes of vertical take-off of rockets and VTOL aircrafts. The regimes for which these base flow characteristics have to be determined are the cases of conventional subsonic and supersonic jet impingement on the flat surface. In the present paper, however, we consider only the case of a plane jet impingement on a flat plate normal to the flow direction.

The flow field can be divided into three regions, the free jet region, the impingement region and the wall jet region. There is a considerable literature available concerning the flow in the free jet region and wall jet region while the impingement region is not yet completely investigated. Experimental results for the impingement region were obtained by Bradshaw and Love (1961) and Schauer and Eustis (1963) which were not verified by theoretical investigations. Tani and Komatsu (1966) and Strand (1962) have obtained the solution to the problem of inviscid jet, impinging normally on to a plate by power series expansion. Recently Wolfshtein (1970) has obtained some interesting numerical solutions for a steady, plane incompressible jet, using finite-difference technique, leaving the heat transfer problem untouched. However, the corresponding unsteady problem including heat transfer has been studied here in the impingement region using the numerical technique due to Dufort and Frankel (1953).

2. Basic Flow Equations

Here, we shall consider the problem of unsteady two-dimensional viscous incompressible jet impingement upon a plate. The governing system of equations are:

Continuity

$$\frac{\partial u}{\partial X} + \frac{\partial v}{\partial Y} = 0 \qquad \ldots(1)$$

Vorticity transport

$$\frac{\partial \Omega}{\partial t} + u\frac{\partial \Omega}{\partial X} + v\frac{\partial \Omega}{\partial Y} = \frac{1}{Re}\left[\frac{\partial^2 \Omega}{\partial X^2} + \frac{\partial^2 \Omega}{\partial Y^2}\right]. \qquad \ldots(2)$$

Energy

$$\frac{\partial \theta}{\partial t} + u\frac{\partial \theta}{\partial X} + v\frac{\partial \theta}{\partial Y} = \frac{1}{RePr}\left[\frac{\partial^2 \theta}{\partial X^2} + \frac{\partial^2 \theta}{\partial Y^2}\right] \qquad \ldots(3)$$

where vorticity

$$\Omega = \frac{\partial v}{\partial X} - \frac{\partial u}{\partial Y}, \quad Re = \frac{U_e D_e}{\nu},$$

$$Pr = \frac{C_p \mu}{\lambda}, \quad \theta = \frac{T - T_w}{T_e - T_w},$$

λ is the heat conductivity, μ the dynamic viscosity, $\nu = \mu/\rho$, T_w the wall temperature (constant) and T_e as well as U_e are also considered to be constant. All velocities are made dimensionless by referring to exist velocity U_e. Temperature and pressure are non-dimensionalized with respect to the exit values T_e and ρU_e^2 respectively, and linear dimensions with respect to the nozzle diameter D_e. The equation of continuity is automatically satisfied by introducing a stream function ψ such that,

$$u = \frac{\partial \psi}{\partial Y}, \quad v = -\frac{\partial \psi}{\partial X} \qquad \ldots(4)$$

where

$$\psi = \int u dy - \int v dx$$

and the stream function ψ is connected with the vorticity function Ω by the equation

$$\Omega = -\left[\frac{\partial^2 \psi}{\partial X^2} + \frac{\partial^2 \psi}{\partial Y^2}\right]. \qquad \ldots(5)$$

3. Boundary Conditions

Figure 1 describes the jet impingement system. We define the boundaries as:

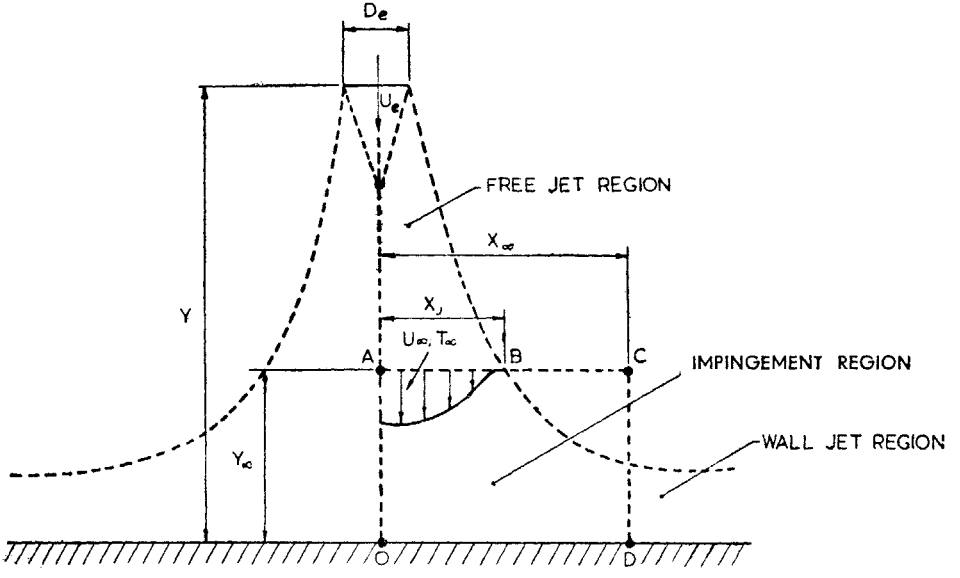

FIG. 1. Schematic diagram of jet impingement.

$$Y_\infty = 1{\cdot}0,\ X_\infty = 2X_j \qquad \ldots(6)$$

where X_j is the free jet thickness at a distance from the nozzle equal to $(Y - Y_\infty)$. From Schauer and Eustis's data (1963) on free jets, X_j is given by

$$X_j = 0{\cdot}22\ (Y - Y_\infty). \qquad \ldots(7)$$

Thus the impingement region with well defined flat surface and the axis of symmetry is bounded by

$$0 \leqslant Y \leqslant Y_\infty = 1{\cdot}0;$$

$$0 \leqslant X \leqslant X_\infty = 2.X_j = 0{\cdot}44\,(Y - Y_\infty). \qquad \ldots(8)$$

Now we define the boundary conditions for the dynamical and heat transfer problems separately for a hot jet impinging on a plate.

Dynamical Problem

On OA : $\psi = 0,\ \Omega = 0,\ \dfrac{\partial \psi}{\partial Y} = 0$ at $t \geqslant 0$

On OD : $\psi = 0,\ \Omega = 0,$ at $t = 0$

$\psi = 0,\ \Omega_0 = -\nabla^2 \psi$ at $t > 0$

On CD : The flow is of boundary layer type, thus

$$\frac{\partial \psi}{\partial X} = \frac{\partial \Omega}{\partial X} = 0 \quad \text{at} \quad t \geqslant 0$$

On BC : The flow is irrotational and the streamlines may be assumed to be parallel to the jet axis, therefore

$$\frac{\partial \psi}{\partial Y} = 0, \quad \Omega = 0 \quad \text{for} \quad t \geqslant 0$$

$$\text{On} \quad AB : \quad \psi = -\int U_\infty \, dX, \quad \Omega = \frac{\partial U_\infty}{\partial X} \quad \text{for all} \quad t \geqslant 0. \qquad \ldots(9)$$

Let U_∞ be determined from the well-known Schlichting's profile for a free jet, thus

$$\frac{U_\infty}{U_{\infty m}} = \left[1 - \left(\frac{X}{X_j}\right)^{3/2}\right]^2 \qquad \ldots(10)$$

where $U_{\infty m}$ is the maximum velocity on the jet axis given by

$$U_{\infty m} = \frac{2 \cdot 35}{(Y - Y_\infty)^{1/2}} .$$

Therefore for Schlichting's profile, the boundary conditions on AB can be written as

$$\psi = - U_{\infty m} X_j \left[\left(\frac{X}{X_j}\right) - 0 \cdot 8 \left(\frac{X}{X_j}\right)^{5/2} + 0 \cdot 25 \left(\frac{X}{X_j}\right)^4\right]$$

$$\Omega = \frac{3 U_{\infty m}}{X_j} \left[\left(\frac{X}{X_j}\right)^2 - \left(\frac{X}{X_j}\right)^{0 \cdot 5}\right]. \qquad \ldots(11)$$

Heat Transfer Problem

For a free two-dimensional jet, we have from Schauer and Eustis (1963)

$$\frac{T - T_a}{T_m - T_a} = \left(\frac{U}{U_m}\right)^{1/2} \qquad \ldots(12)$$

where T_a is the ambient temperature, T_m and U_m are the maximum values of the temperature and velocity on the jet axis. T_m is a function of the distance from the exit section of the nozzle and the exit temperature. Hence, we may write with the help of equation (10).

$$\frac{T_\infty - T_a}{T_{\infty m} - T_a} = \left[1 - \left(\frac{X}{X_j}\right)^{3/2}\right]. \qquad \ldots(13)$$

Following Schauer and Eustis (1963), we have

$$T_{\infty m} - T_a = \frac{2 \cdot 02 \, (T_e - T_a)}{(Y - Y_\infty)^{1/2}} . \qquad \ldots(14)$$

Thus the new variable θ at $Y = Y_\infty$ denoted by θ_∞ with the help of equations (13) and (14) is given by

$$\theta_\infty = \frac{T_\infty - T_w}{T_e - T_w} = \left(\frac{T_e - T_a}{T_e - T_w}\right)\left(\frac{2 \cdot 02}{(Y - Y_\infty)^{1/2}}\right)\left[1 - \left(\frac{X}{X_j}\right)^{3/2}\right]$$

$$+ \frac{T_a - T_w}{T_e - T_w}, \quad \text{for} \quad 0 \leqslant X \leqslant X_j$$

and

$$\theta_\infty = \frac{T_a - T_w}{T_e - T_w}, \quad \text{for} \quad X > X_j. \qquad \ldots(15)$$

But the wall temperature is normally determined from the consideration of the heat balance on the wall surface and therefore varies from plate to plate. Thus for a hot jet and a cold plate; $T_w = T_a$. Now the boundary conditions for the heat transfer problem are specified as follows:

On AB *i.e.* for $0 \leqslant X \leqslant X_j$

$$\theta_\infty = \frac{2{\cdot}02}{(Y - Y_\infty)^{1/2}}\left[1 - \left(\frac{X}{X_j}\right)^{3/2}\right];$$

On BC *i.e.* for $X_j < X \leqslant \lambda_\infty$

$$\theta_\infty = 0, \quad \text{for all} \quad t \geqslant 0;$$

On the wall OD $T = T_w$

$$\theta = \theta_w = 0 \quad \text{for all} \quad t \geqslant 0;$$

On CD we assume the usual boundary layer behaviour

$$\frac{\partial \theta}{\partial X} = 0 \quad \text{for all} \quad t \geqslant 0;$$

On OA the axis of symmetry, we assume

$$\frac{\partial \theta}{\partial X} = 0 \quad \text{for all} \quad t \geqslant 0. \qquad \ldots(16)$$

4. Difference Equations

The numerical technique employed in this paper is due to Dufort and Frankel (1953). We divide the region of computation OABCDO into meshes. After discretization equations (5), (2) and (3) assume the following form:

$$\psi_{i,j}(t) = [(\psi_{i+1,j} + \psi_{i-1,j})\,\triangle Y^2 + (\psi_{i,j+1} + \psi_{i,j-1})\,\triangle X^2 + \Omega_{i,j}\,\triangle X^2\,\triangle Y^2]/2\,(\triangle X^2 + \triangle Y^2). \qquad \ldots(17)$$

The vorticity transport equation is:

$$\Omega^{n+1}_{i,j}\left[\frac{Re}{2\triangle t} + \frac{1}{\triangle X^2} + \frac{1}{\triangle Y^2}\right] = \Omega^{n-1}_{i,j}\left[\frac{Re}{2\triangle t} - \frac{1}{\triangle X^2} - \frac{1}{\triangle Y^2}\right] + \frac{Re}{4\triangle X \triangle Y}[(\psi^n_{i+1,j} - \psi^n_{i-1,j})(\Omega^n_{i,j+1} - \Omega^n_{i,j-1}) - (\psi^n_{i,j+1} - \psi^n_{i,j-1})(\Omega^n_{i+1,j} - \Omega^n_{i-1,j})] + (\Omega^n_{i+1,j} + \Omega^n_{i-1,j})/\triangle X^2 + (\Omega^n_{i,j+1} + \Omega^n_{i,j-1})/\triangle Y^2. \qquad \ldots(18)$$

The energy equation is

$$\theta_{i,j}^{n+1}\left[\frac{RePr}{2\triangle t}+\frac{1}{\triangle X^2}+\frac{1}{\triangle Y^2}\right]=\theta_{i,j}^{n-1}\left[\frac{RePr}{2\triangle t}-\frac{1}{\triangle X^2}-\frac{1}{\triangle Y^2}\right]$$

$$+\frac{RePr}{4\triangle X\triangle Y}[(\psi_{i+1,j}^{n}-\psi_{i-1,j}^{n})(\theta_{i,j+1}^{n}-\theta_{i,j-1}^{n})$$

$$-(\psi_{i,j+1}^{n}-\psi_{i,j-1}^{n})(\theta_{i+1,j}^{n}-\theta_{i-1,j}^{n})]$$

$$+(\theta_{i+1,j}^{n}+\theta_{i-1,j})/\triangle X^2+(\theta_{i,j+1}^{n}+\theta_{i,j-1})/\triangle Y^2. \qquad ...(19)$$

Here, the subscripts i and j correspond to the x and y coordinates, while the superscript n indicates the time index and not a power. This type of discretization gives a better computationally stable scheme which was first suggested by Dufort and Frankel (1953).

5. Numerical Method

The general computational method is described here:

(i) Since the flow starts impulsively from rest and is irrotational, the initial values of ψ, Ω and θ have been set to zero at all mesh points except on AB where ψ, Ω and θ are computed using equations (11) and (16).

(ii) Equation (17) has been solved using over-relaxation method to obtain improved stream function values at all interior mesh points. The iterative method is assumed to converge when the current values ψ^{r+1} differ by less than 10^{-6} from past values ψ^{r} at all mesh points. Using the over-relaxation scheme, equation (17) is rewritten as

$$\psi_{i,j}^{(r+1)}=\psi_{i,j}^{(r)}+W[\{(\psi_{i+1,j}^{*}+\psi_{i-1,j}^{*})\triangle Y^2+(\psi_{i,j+1}^{*}+\psi_{i,j-1}^{*})\triangle X^2$$

$$+\Omega_{i,j}\triangle X^2\triangle Y^2\}/2(\triangle X^2+\triangle Y^2)-\psi_{i,j}^{(r)}]. \qquad ...(20)$$

Here, W is the over-relaxation factor, and superscripts (r) and $(r+1)$ indicate the values at the rth and $(r+1)$th iteration respectively; superscript * indicates the most recent corrected value. After some preliminary tests the value of W has been fixed at 1·85.

(iii) Knowing ψ, the wall vorticity Ω_0 is computed from

$$\Omega_0=2[\psi_{i,NJ}-\psi_{i,NJ-1}]/\triangle Y^2$$

where the subscript NJ corresponds to the wall.

(iv) The non-dimensional time has been advanced by $\triangle t$ and at this new time $t=\triangle t$, the vorticity Ω and temperature θ are computed at all the interior points using equations (18) and (19).

(v) Steps (ii) to (iv) at time $t = \triangle t$ are repeated. These steps have been further repeated at latter times. At selected time intervals the static pressure distribution on the wall and shear stress on the surface of the wall have been computed using the following:

Pressure distribution on the wall—The momentum equation gives

$$\frac{\partial p}{\partial x}\bigg|_{y=0} = -\frac{1}{Re}\frac{\partial \Omega}{\partial Y}\bigg|_{y=0}.$$

The static pressure $[p(x) - p_\infty]$ on the wall has been computed from

$$[p(x) - p_\infty) = U_{\infty m}^2 - \frac{1}{Re}\int_0^X \left(\frac{\partial \Omega}{\partial y}\right) dX\bigg|_{y=0}. \qquad \ldots(21)$$

Shear stress on the wall—The non-dimensional value of the shear stress τ_w has been obtained from the following equation, namely

$$\tau_w = \frac{1}{Re}\left(\frac{\partial^2 \psi}{\partial X^2} + \frac{\partial^2 \psi}{\partial Y^2}\right)\bigg|_{y=0}. \qquad \ldots(22)$$

Nusselt number distribution—The distribution of the Nusselt number on the wall surface is

$$Nu = \frac{\partial \theta}{\partial Y}\bigg|_{Y=0}. \qquad \ldots(23)$$

Besides, the variation of the radial velocity u close to the surface and the vertical velocity — v along the jet axis are also computed and printed.

The numerical calculations were done on high speed digital computer IBM 360/44 system. Machine time required to complete computations for a typical case $Re = 450$, $\triangle t = 0{\cdot}02$, $\triangle X = 0{\cdot}016$, $\triangle Y = 0{\cdot}05$ (upto $t = 24$) was about 3 hours. Some numerical tests were made to test the effects of $\triangle X$, $\triangle Y$, $\triangle t$. At $Re = 450$, the computer program was run upto $t = 4$ with fixed $\triangle t = 0{\cdot}02$ and $\triangle X = 0{\cdot}008$, $\triangle Y = 0{\cdot}025$. The time consumed was almost double when compared with the former case while the improvement in the results of pressure distribution on the wall, shear stress on the wall, etc., had not been very much. Then $\triangle t$ was taken equal to $0{\cdot}02$ and $0{\cdot}01$ and the results were compared at $t = 4$, 8 and 9. At $t = 4$ and 8 the absolute difference between the computed values for the two cases was found to be less than 10^{-3} and less than 10^{-4} at $t = 9$. These tests enabled us to choose $\triangle t = 0{\cdot}02$, $\triangle X = 0{\cdot}016$, $\triangle Y = 0{\cdot}05$ and the program was run upto $t = 24$ at $Re = 450$.

Still higher values of Re are not chosen in our investigations in view of the well-known fact that the Dufort-Frankel method develops persistent oscillations as a steady state is approached at high Reynolds numbers. Development of higher order numerical schemes to deal with high Reynolds numbers is under progress.

6. Numerical Results

Figure 1 illustrates the geometry and boundary conditions of our problem. Here, we present the numerical results of the impinging jet problem described in Sections 2 and 3, for the following main jet parameters, namely Reynolds number (Re) = 450, Prandtl's number (Pr) = 1·0, the nozzle to control surface spacing ($Y - Y_\infty$) = 8, 12 and 16.

Figures 2 – 8 illustrate various flow characteristics for $Re = 450$, $Y - Y_\infty = 16$,

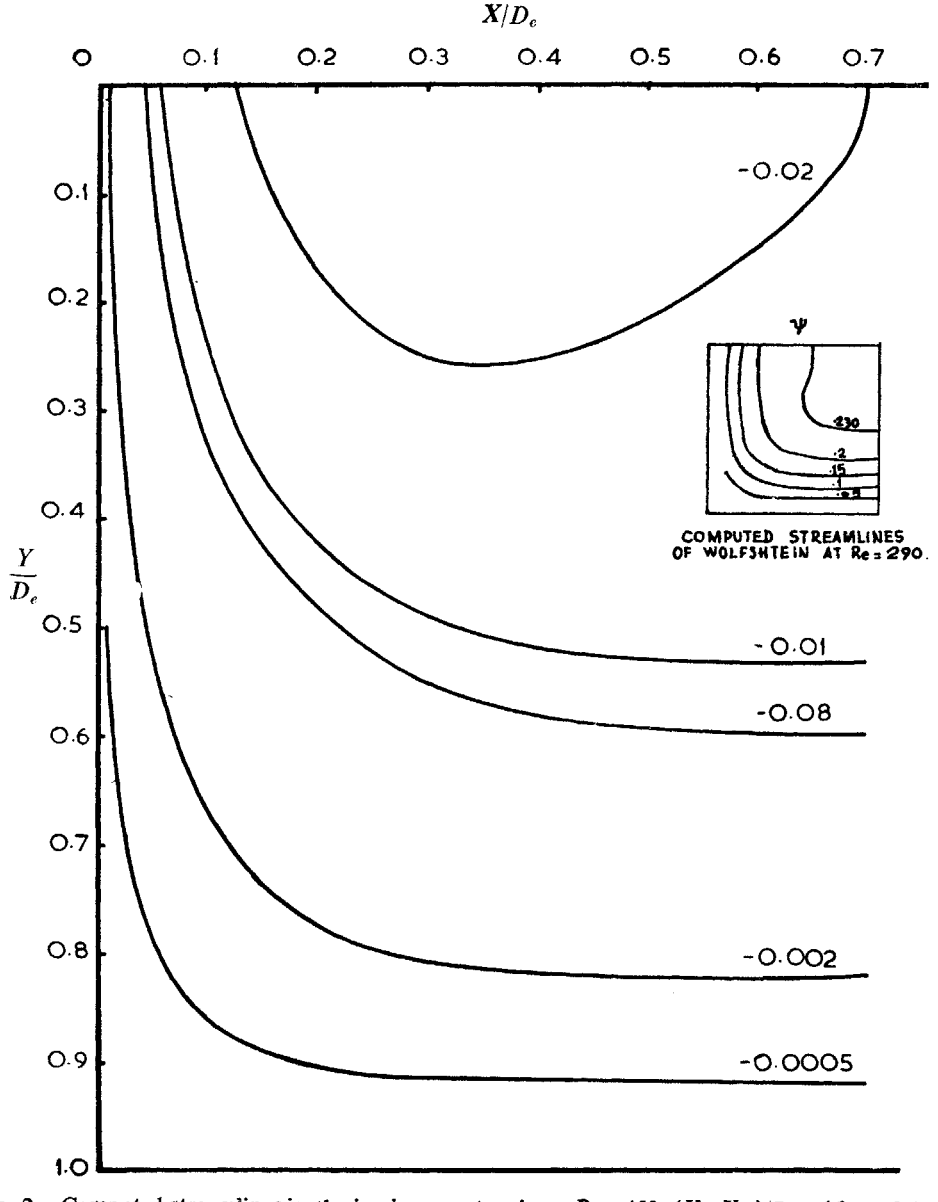

FIG. 2. Computed streamlines in the impingement region. $Re = 450$, $(Y - Y_\infty)/D_e = 16$, $t = 6{\cdot}0$.

$\triangle t = 0{\cdot}02$, $\triangle X = 0{\cdot}016$, $\triangle Y = 0{\cdot}05$. Streamlines and equivorticity lines are shown in Figs. 2 and 3, respectively. The streamlines have large curvature

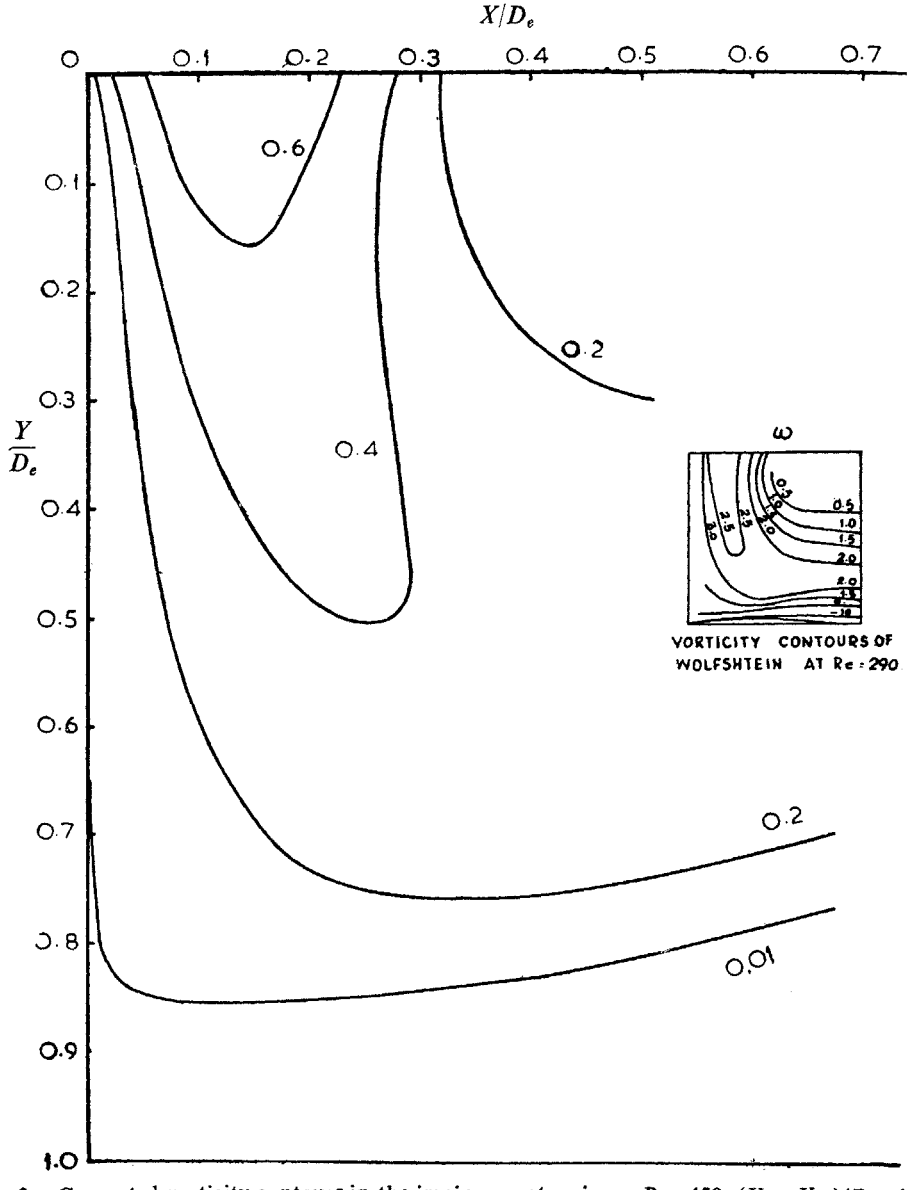

FIG. 3. Computed vorticity contours in the impingement region. Re=450, $(Y - Y_\infty)/D_e$=16, $t = 24{\cdot}0$.

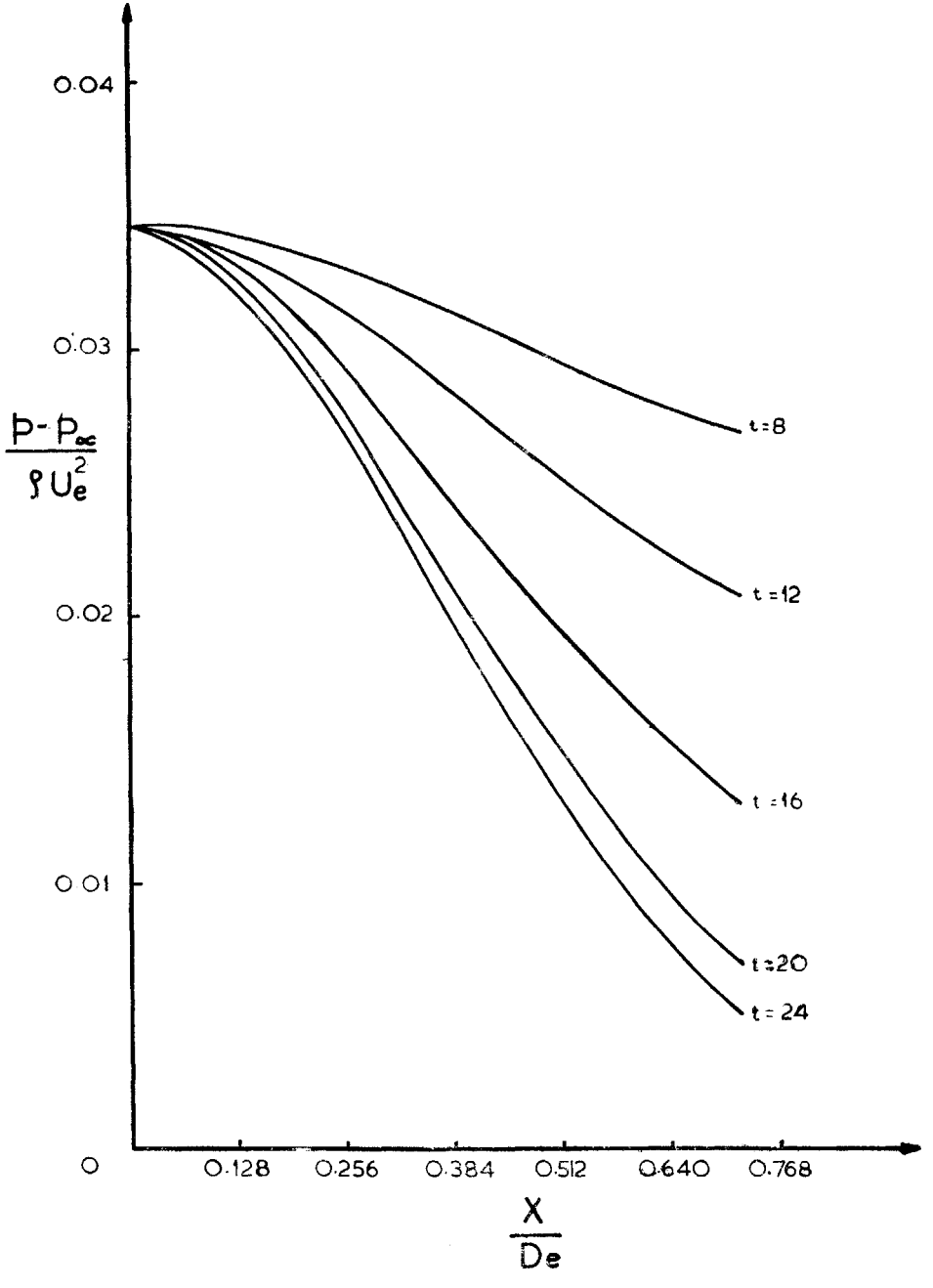

FIG. 4. The static pressure distribution on the wall. $Re = 450$, $(Y - Y_\infty)/D_e = 16$.

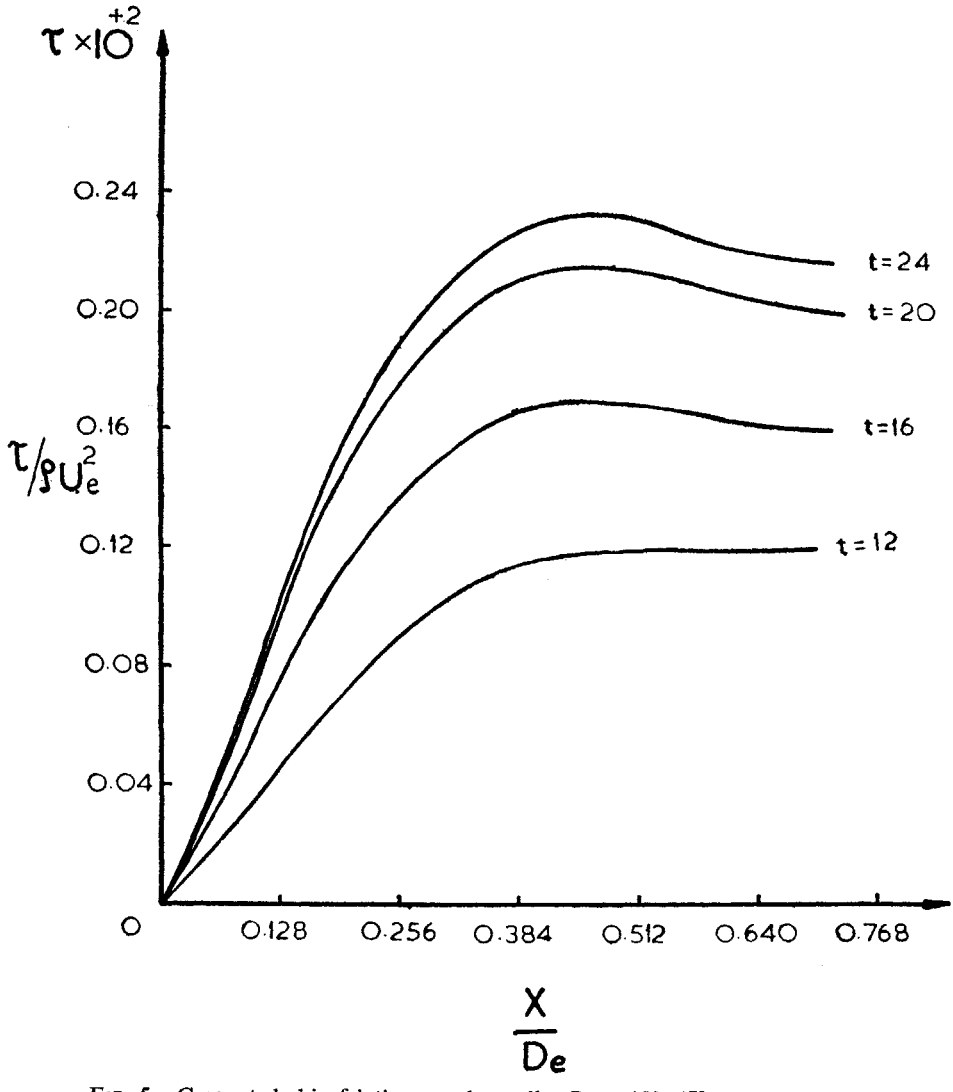

FIG. 5. Computed skin friction on the wall. $Re = 450$, $(Y - Y_\infty)/D_e = 16$.

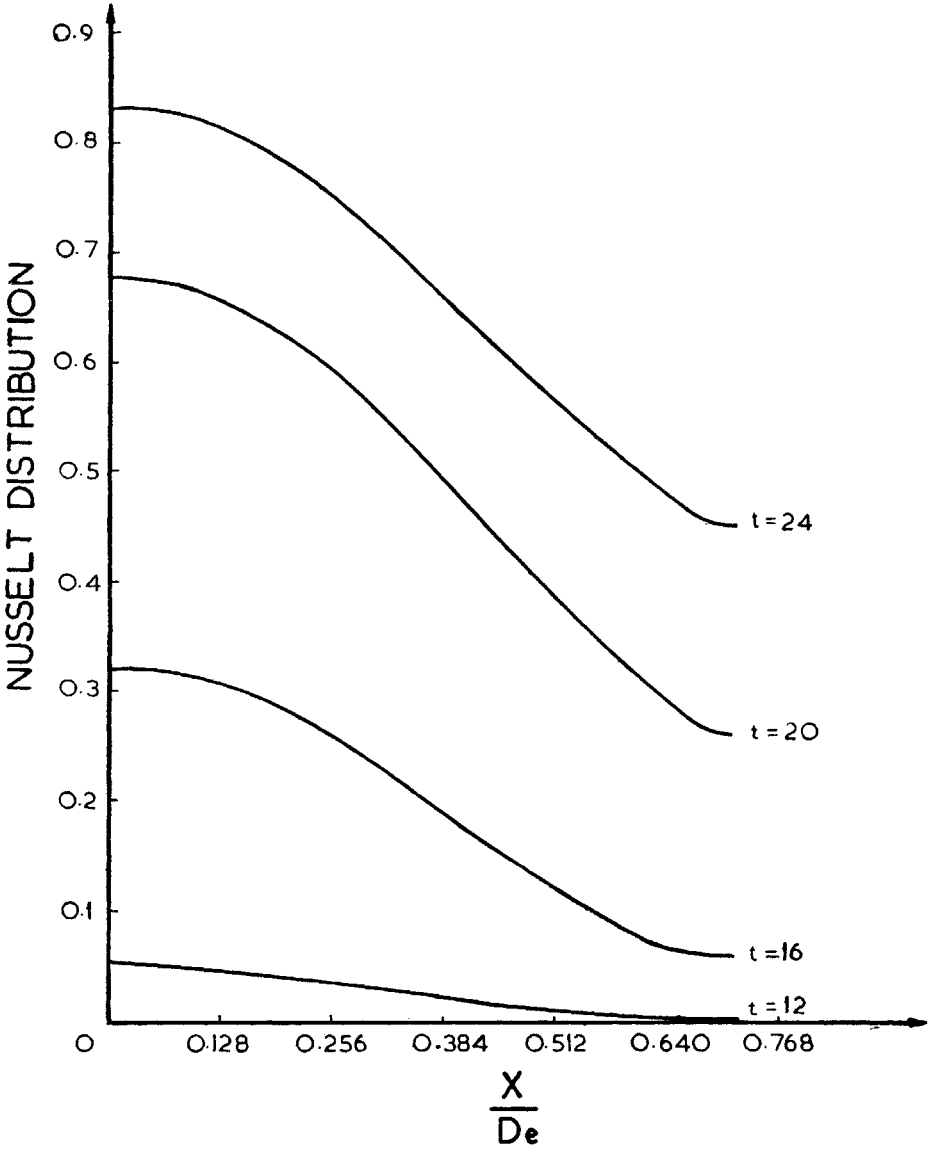

FIG. 6. Computed Nusselt number distribution on the wall. $Re = 450$, $(Y - Y_\infty)/D_e = 16$.

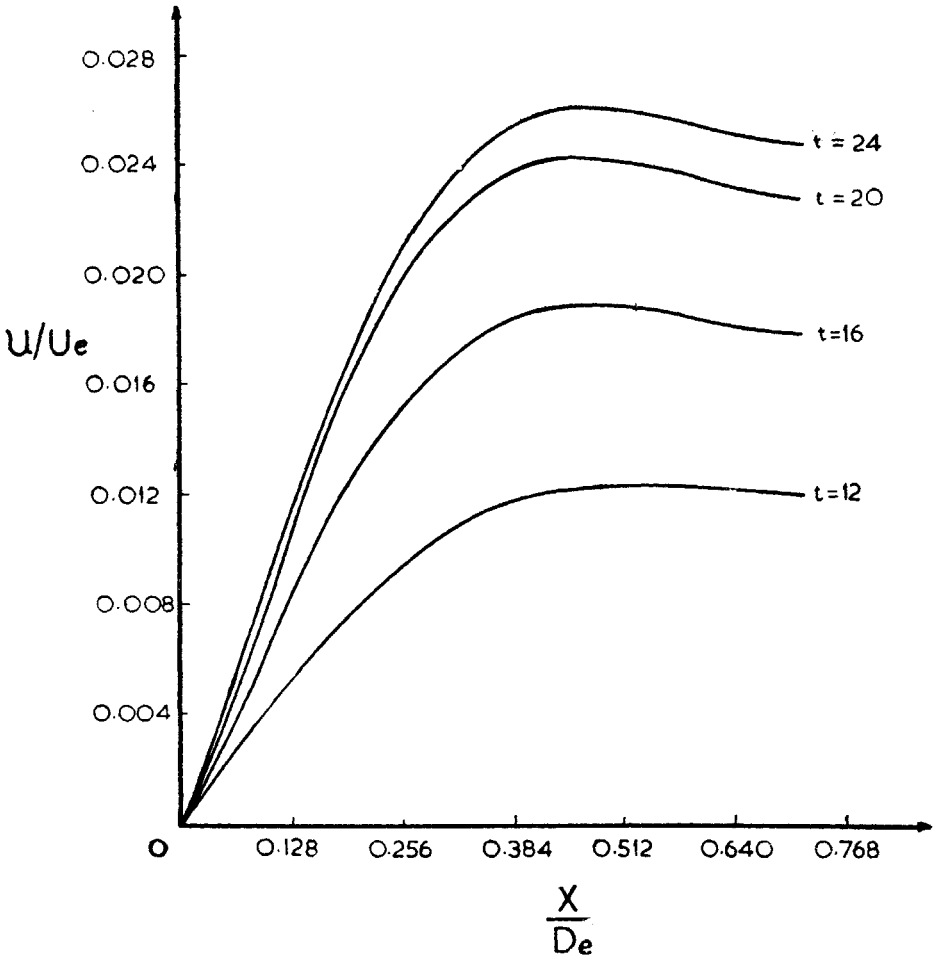

FIG. 7. Variation of radial component of the velocity u/U_e close to the wall $Re = 450$, $(Y - Y_\infty)/D_e = 16$.

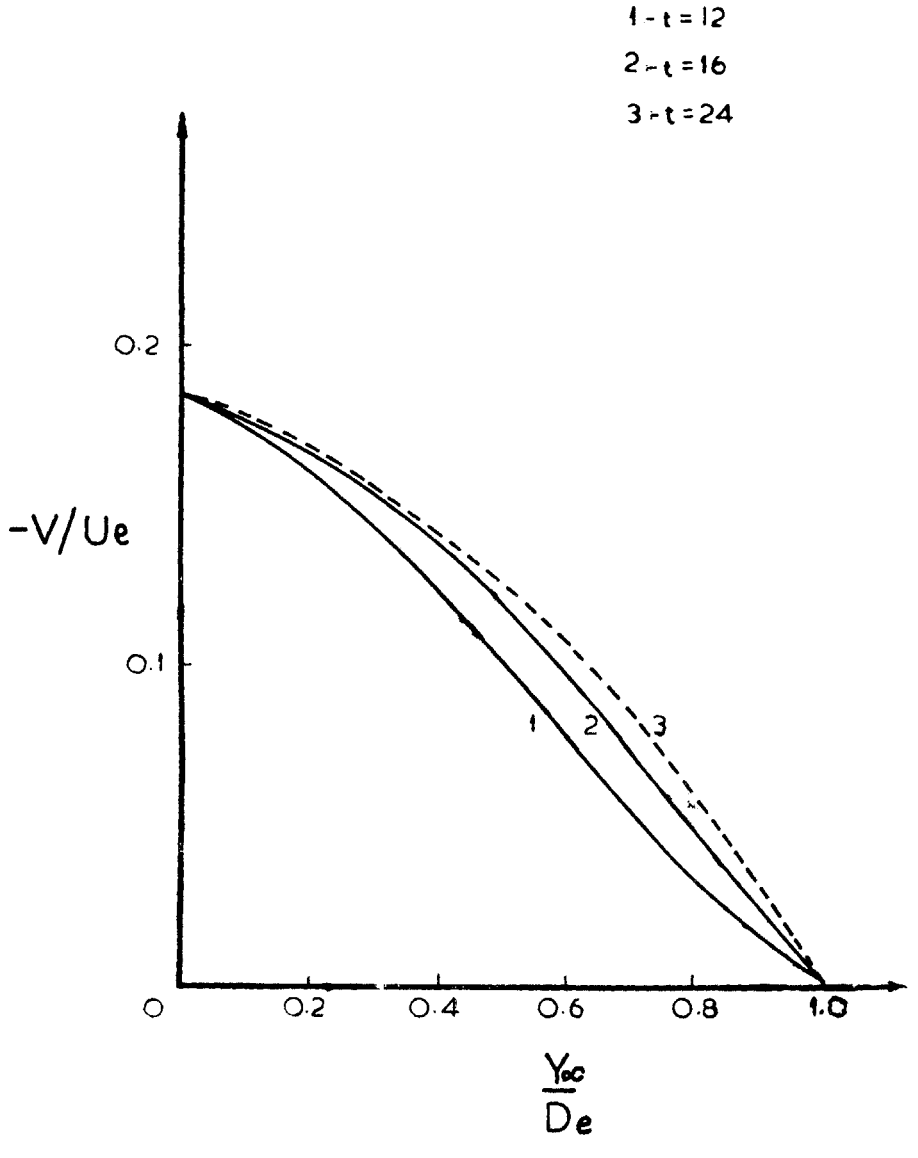

FIG. 8. Variation of vertical velocity $-v/U_e$ along the jet centre line. $Re = 450$, $(Y - Y_\infty)/D_e = 16$.

near the stagnation point which is associated with high pressure gradients. Another interesting feature is that equivorticity lines are nearly parallel to the streamlines. This indicates the slow variation of vorticity along the streamlines. In this connection, we mention the results of Wolfshtein (1970) who has plotted the streamlines for $Re = 290$ for the separation distance $Y - Y_\infty = 16$ (*see* the insert in Figs. 2 and 3). A comparison of the streamlines and equivorticity lines obtained by us with Wolfshtein are in qualitative agreement.

The non-dimensional pressure distribution $(p - p_\infty)$ on the wall is plotted as shown in Fig. 4 with time 't' as parameter. It can be seen that a steady state solution is reached at $t = 24$. The pressure falls with distance along the wall from the maximum value p_0 at the stagnation point to p_∞.

Figures 5 and 7 show the skin friction distribution on the surface of the wall and the variation of radial component of velocity u with x in the vicinity of the wall. Both τ and u are found to increase sharply under the influence of the pressure gradient from zero at the stagnation point and then falls off due to viscous dissipation. Figure 6 depicts the behaviour of the Nusselt number distribution in the impingement region for $(Y - Y_\infty) = 16$ and $Re = 450$. We find a bell-shaped nature with peak value at stagnation point; which is the characteristic of a fully developed air jet.

Figure 8 shows the distribution of the vertical velocity $-v$ along the jet centre line at various times as the flow develops. It has the tendency of falling and finally becoming zero at the stagnation point.

ACKNOWLEDGEMENT

The author would like to acknowledge the many valuable discussions he had with Professor I. A. Belov of Mechanical Institute, Leningrad, during the development of this work. The help of Miss Leelamma Simon in computing the numerical results is gratefully acknowledged. The author is also thankful to the referee for his useful comments.

REFERENCES

Bradshaw, P., and Love, E. M. (1961). The normal impingement of a circular air jet on a flat surface. *A.R.C.R. and M. No.* 3205.

Dufort, E. C., and Frankel, S. P. (1953). Stability conditions in the numerical treatment of parabolic differential equations. *Math. Tables Aids Comput.*, **7**, 135.

Jain, P. C., and Sankara Rao, K. (1969). Numerical solution of unsteady viscous incompressible fluid flow past a circular cylinder. *Phys. Fluids, Supplement II*, **12**, 57.

Schauer, J. J., and Eustis, R. H. (1963). The flow development and heat transfer characteristics of plane turbulent impinging jets. *Dept. Mech. Engng. TR No.* 3.

Strand, T. (1962). Inviscid-incompressible flow theory of static two-dimensional solid jets in proximity to the ground. *J. Aero. Sci.*, **29**, 170.

Tani, I., and Komatsu, Y. (1966). Impingement of a Round Jet on a Flat Surface. Springer Verlag, New York, p. 672.

Wolfshtein, M. (1970). Some solutions of the plane turbulent impinging jet. *Trans. ASME J. Basic Engng., Paper No.* 70-*FE*-27, 1.